Theory of hydrogen in diamond

J. P. Goss and R. Jones
School of Physics, Stocker Road, University of Exeter, Exeter, Devon, EX4 4QL, United Kingdom

M. I. Heggie and C. P. Ewels
CPES, University of Sussex, Falmer, Brighton, BN1 9QJ, United Kingdom

P. R. Briddon
Department of Physics, University of Newcastle upon Tyne, Newcastle upon Tyne, NE1 7RU, United Kingdom

S. Öberg
Department of Mathematics, Luleå University of Technology, SE-971 87 Luleå, Sweden
(Received 7 June 2001; published 4 March 2002)

Ab initio cluster and supercell methods are used to investigate the local geometry and optical properties of hydrogen defects in diamond. For an isolated impurity, the bond-centered site is found to be lowest in energy, and to possess both donor and acceptor levels. The neutral defect possesses a single local mode with a very small infrared effective charge, but the effective charge for the negative charge state is much larger. H^+ is calculated to be very mobile with a low activation barrier. Hydrogen dimers are stable as H_2^* defects, which are also found to be almost IR inactive. The complex between B and H is investigated and the activation energy for the reaction B-H$\rightarrow B^- + H^+$ found to be around 1.8 eV in agreement with experiment. We also investigate complexes of hydrogen with phosphorus and nitrogen. The binding energy of H with P is too low to lead to a significant codoping effect. A hydrogen-related vibrational mode of the N-H defect, and its isotopic shifts, are close to the commonly observed 3107-cm^{-1} line, and we tentatively assign this center to the defect. Hydrogen is strongly bound to dislocations which, together with H_2^*, may form part of the hydrogen accumulation layer detected in some plasma studies.

DOI: 10.1103/PhysRevB.65.115207 PACS number(s): 78.20.Bh, 61.72.Bb, 71.55.Cn

I. INTRODUCTION

Hydrogen is a ubiquitous impurity in diamond, but unlike other group-IV materials, there is little detailed information about any hydrogen defect. This is to be contrasted with silicon, where a great wealth of details regarding H centers exists. For example, in Si, isolated neutral-bond centered H defects have been observed[1,2] by electron paramagnetic resonance (EPR), after low-temperature proton implantation and illumination with band-gap light. Isolated H is a negative-U defect with a donor level at $E_c - 0.175$ eV,[3] and an acceptor level, due to a structure when H lies at an antibonding or tetrahedral interstitial site, at $E_c - 0.5$ eV.[4–6] A vibrational mode at 1998 cm^{-1} is attributed to H^+ at a bond center,[7] but no local modes are known for the neutral or negative species. The center is mobile, with a migration barrier of around 0.4 eV,[8] and the defect anneals around 200 K.

Hydrogen dimers have been predicted to exist as H_2 molecules[9] and H_2^* defects,[10] and both defects have been observed in infrared-absorption experiments.[11,12] The solubility of hydrogen in silicon is activated with an energy around 1.8 eV.[13] In addition, there are numerous complexes containing hydrogen, such as vacancies,[7,14] interstitials,[15] and impurities. Many of these have been characterized by local mode spectroscopy.

The situation regarding diamond is very different. Muon implantation experiments[16] and theory[17–21] both indicate that neutral hydrogen is metastable at a tetrahedral interstitial site, with its lowest energy configuration consisting of hydrogen at or around the bond center. Although there are many IR-absorption peaks seen in diamond with frequencies in the range expected for C-H stretch modes, none of them are understood. A commonly detected mode in natural material lies at 3107 cm^{-1}, but this cannot be due to on-axis bond-centered hydrogen with D_{3d} symmetry, as the defect does not possess inversion symmetry,[22] and involves only one carbon atom.[23] Although stress measurements have been made on the line, no splittings were resolved,[24] and the point group symmetry is not known. The involvement of nitrogen in this defect was ruled out because there is no significant change in its frequency with ^{15}N.[23] However, more correctly this means that the effect of any nitrogen in the defect is unresolved. It was suggested[24,25] that the concentration of centers giving rise to the 3107-cm^{-1} band in natural material cannot account for all the hydrogen which can reach 1 at % in some natural[26] and polycrystalline chemical vapor deposition (CVD) [Ref. 27] diamonds. Thus it seems highly likely that hydrogen is incorporated in other forms, and it has been suggested that the hydrogen is contained within inclusions,[28] grain boundaries, and dislocations.[27]

Electron paramagnetic resonance has revealed a defect labeled H1 attributed to a dangling bond on carbon near hydrogen and located within or close to grain boundaries.[29,30] The total infrared absorption in the 2750–3300 cm^{-1} range associated with C-H stretch modes correlates[30] with the concentration of H1, implying that most of the IR-active hydrogen in polycrystalline CVD material is associated with intergranular regions; however, this does not rule out the presence

of IR-invisible, diamagnetic hydrogen within crystals. Furthermore, there is a number of electronic transitions associated with the presence of hydrogen, such as the absorption peak at ~ 0.9 eV,[23] although, to the knowledge of the authors, none has been correlated with IR studies or even with a specific defect.

Impurities and lattice defects might be expected to trap hydrogen, but boron is the only known example to date. The correlation between the secondary ion mass spectroscopy (SIMS) profiles of deuterium, introduced by a plasma, and B in polycrystalline CVD material suggest that a single deuterium atom is complexed with boron. The loss of the electronic IR absorption due to the substitutional B acceptor implies that boron is passivated.[31–33] These experiments were carried out on polycrystalline CVD diamond doped with boron. Both radio frequency (rf) and microwave (mw) plasmas were used to introduce deuterium, with the latter being a much less aggressive method, leading to lower levels of incorporated deuterium. For the mw plasma and temperatures $\leqslant 550\,^{\circ}$C, the deuterium penetrated about 0.27 μm and closely followed the B profile consistent with the formation of B-D. For higher temperatures, deeper penetrations of ~ 1 μm were observed and only a fraction of boron remains passivated. An estimate of the energy barrier to the dissociation of B-D comes from the activation energy for the diffusion, of D as measured by the increase in penetration depth above 550 °C. This yields a barrier of 1.43 eV.

In the rf plasma, an accumulation layer containing $\sim 10^{22}$ cm^{-3} of deuterium extending to depths about 0.1 μm is formed. This suggests that H introduced by the rf plasma can create lattice damage or is self-trapped by forming stable multihydrogen centers. Heating to temperatures $\geqslant 290\,^{\circ}$C liberates this hydrogen, whose diffusion is not limited by boron trapping since it exceeds the concentration of boron. The temperature dependence of the penetration depth shows that diffusion is now activated with an energy of only 0.35 eV, and may be related to the migration of free H^+. Hydrogen effusion experiments indicated that the adsorbed surface hydrogen was lost at 850 °C and the hydrogen in the accumulation layer at 720 °C. The closeness in these temperatures suggests that at least some of the hydrogen in the accumulation layer is in the form of C-H bonds possibly in near-surface cracks. Capacitance-voltage studies on a high-pressure synthetic diamond doped with boron, into which deuterium had been introduced by a plasma, also demonstrated that B is passivated.[34]

This accumulation of hydrogen in the subsurface region is seen in all hydrogenated material.[32,33,35–37] Samples that have been hydrogenated exhibit a *p*-type near-surface conductivity, with a hole activation energy an order of magnitude lower than that of boron. Several models have been proposed for the source of the conductivity. One suggestion is that hydrogen is directly responsible for the acceptor level,[35] although it is hard to understand how any point defect could give rise to such a shallow level. A more likely model involves the transfer of electrons from diamond to surface adsorbates,[38–40] but the experimental evidence is far from clear. As a final point, it has been suggested that hydrogen introduced by implantation *self-traps*,[41] implying the simultaneous formation of an immobile hydrogen aggregate or a lattice defect.

In this paper we present the results of first-principles calculations regarding the structure and experimental observables associated with simple forms of hydrogen in diamond. Previous theory produced a range of structures and migration barriers for isolated hydrogen in diamond. Early calculations[17–19] showed that the presence of hydrogen in the bond-centered location tends to push the surrounding lattice apart. However, the energy associated with this strain is more than compensated for by the strong chemical bonding, giving a saving in energy of around 2–3 eV (Ref. 18) relative to the tetrahedral site. An axial, bond-centered geometry (trigonal symmetry) is preferred by most theories, although recent semiempirical calculations[21] suggested an off-axis defect termed the ''equilateral triangle'' (ET) model. The barrier to migration for bond-centered hydrogen was estimated at 0.9 eV (Ref. 21) and around 2 eV,[20,42] with the positive charge state being much more mobile.[43]

Models for two nearby hydrogen atoms include the H_2^* complex, a molecule or the bridge defect made up from the two H atoms sharing a single C-C bond. In contrast to other group-IV materials, theory suggests that the molecule is not the lowest-energy form in diamond, with H_2^* lying 3.3 eV lower in energy,[19] or between 1.5 (Ref. 20) and 3.5 eV (Ref. 19) lower than two separated bond-centered hydrogen defects.

The structure of the the B-H pair in diamond is quite different from silicon.[44,43] In diamond, the H atom lies approximately 1.1–1.2 Å along the [001] direction from B, but is displaced closer to one of the two carbon neighbors of boron along this direction (see Fig. 9). Previous calculations[43] found the activation energy for the dissociation of boron-hydrogen pairs to be 0.3 eV. They also found that a free H atom outside diamond was 1.54 eV higher in energy than H bound to substitutional B, implying that boron has a large effect on the solubility of hydrogen.

In Sec. II, we briefly discuss details of the method of calculation, and we describe results on isolated hydrogen centers in Sec. III. Section IV discusses the solubility of hydrogen in diamond, while Secs. VI and VII deal with hydrogen dimers, H-B, H-N, and H-P centers. Finally, the interaction of hydrogen with dislocations is dealt with in Sec. VIII.

II. METHOD

Local-density-functional calculations using both cluster and supercell methods were carried out on hydrogen defects using the AIMPRO code.[45,46] Previously, the method was used to successfully explore the properties of nitrogen aggregates[47], N*V* and Si*V* defects.[48] divacancies,[49] and interstitial aggregates in diamond.[50]

Where appropriate, the symmetry of the defect has been constrained during the relaxation. Calculations employed hydrogen-terminated clusters ranging from $C_{68}H_{66}$ to $C_{181}H_{116}$, or 64-atom cubic unit cells into which the interstitial hydrogen atoms were placed. The atoms are treated using the pseudopotentials of Ref. 51, except for hydrogen, where

the bare Coulomb potential is used. The convergence with unit cell size was tested by relaxing H_2^* defects in 64- and 216-atom unit cells. The differences in bond lengths were less than 0.2%, and the absolute formation energy differed by around 0.2 eV.

Two types of basis were used for the supercell calculation. The first consists of independent *s*, p_x, p_y, and p_z Gaussian orbitals with four different exponents, sited at each C site, and two exponents at the central hydrogen atoms. In addition, a set of *s* and *p* Gaussian orbitals was placed at each C-C bond center. The second consisted of *s*, *p*, and *d* Gaussian functions centered at the atomic sites with four exponents. The advantage of the basis set with bond-centered functions is the smaller computational effort, but the number and location of the bond-centered functions varies with different structures. This disadvantage is removed by using a basis set including *d* functions at the atom sites, but the computational effort is increased. The difference in relative total energies using different basis sets, is generally found to be small (typically a few tenths of an eV), except for a few cases where in both basis sets the structures are high in energy relative to the ground state. Both basis sets yield lattice constants and bulk moduli within around 1% and 5%, respectively, of the experimental values. The direct and indirect band gaps are in close agreement with the local-density-approximation values of Liberman[52] (5.68 and 4.18 eV).

For clusters the wave functions were expanded using a similar basis to the first type employed in the supercell. A fixed linear combination of two Gaussian orbitals is sited on the terminating H atoms, and the charge density is fitted with four (three) independent *s* Gaussian functions with different widths on each C(H) atom. One extra *s* Gaussian function is placed at each C-C bond center. Supercell calculations were carried out using an MP-2^3 set of **k** points to sample the band structure. The charge density is Fourier transformed using plane waves with a cutoff of 120 Ry.

Local vibrational modes can be estimated using standard techniques, with the dynamical matrix being constructed using a mixture of calculated values of the energy double derivatives in the region of the defect, with other regions using terms generated from valence force potential.

The measured intensity of infrared absorption for a given mode is related to the effective charge of the oscillator η, where

$$\eta^2/m = \frac{1}{3}\sum (\partial \mathbf{M}/\partial Q)^2.$$

Here *m* is the mass of the oscillator, **M** is the induced dipole caused when the atoms are displaced according to their normal coordinates, and *Q* is the amplitude of the mode. The sum is over *x*, *y*, and *z* and over any mode degeneracy.[53] For silicon, the experimentally measured value of η for the positively charged bond-centered interstitial hydrogen defect is $3e$ taking $m=1$.[7,54] Previous theoretical calculations using AIMPRO (Ref. 55) yielded a value $\sim 1e$, considerably smaller than experiment showing the difficulty in evaluating this parameter. The calculated values of experimentally observable parameters quoted in the text are taken from the supercell method except where stated otherwise, while the effective charges are found using the cluster method.

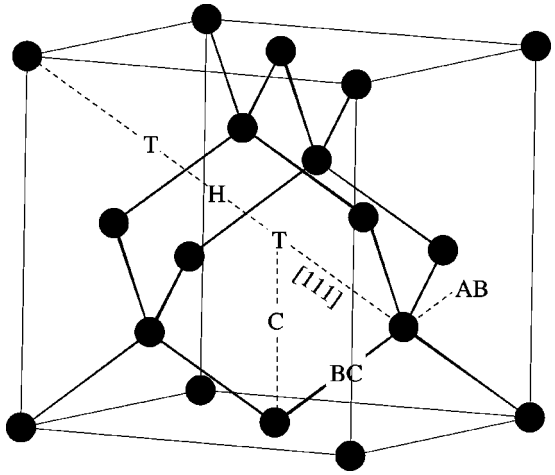

FIG. 1. Schematic showing the bond-centered (BC), anitbonding (AB), tetrahedral (*T*), hexagonal (*H*), and *C*-site interstitial sites in diamond. The *H* and *T* sites lie halfway and a third of the way along the line joining two atoms along the [111] direction. The *C* site is midway between an atom site and a neighboring *T* site.

III. ISOLATED HYDROGEN CENTERS

The energy and structures of interstitial hydrogen at several sites in the diamond lattice, and in a number of charge states, were calculated using both supercells and clusters. The sites considered were the tetrahedral (*T*), and hexagonal (*H*), *C* sites, the bond-centered (BC) sites, and the antibonding site (Fig. 1). For completeness, the BC structure was relaxed using different starting configurations where the H atom lay on and off the bond axis. Table I lists the relative total energies for each structure in the neutral, negative, and positive charge states found using a supercell. The energies found using clusters are very similar. As can readily be seen, the BC location is found to be the lowest energy site for the neutral and negative defects, while the puckered BC location is the most stable in the positive charge state. We relaxed the ET structure of Ref. 21 in all charge states. In all cases the H atom returned to a location equidistant from two carbon nearest neighbors. We suppose that this structure is an artifact of the semiempirical technique used.

TABLE I. Relative total energies (supercell) of the single interstitial H defect in diamond (eV). The zero of the energy scale for each charge state is taken to be the energy of the most stable structure examined in this study.

Structure	Symmetry	1+	0	1−
Bond-centered	D_{3d}	0.3	0.0	0.0
Puckered bond-center	$C_2/C_{1h}/C_1$	0.0	unstable	unstable
Anit-bonded	C_{3v}	0.4	unstable	1.2
C site	C_{2v}	0.0	unstable	unstable
Hexagonal site	D_{3d}	0.2	1.7	3.0
Tetrahetral site	T_d	0.6	1.0	1.5

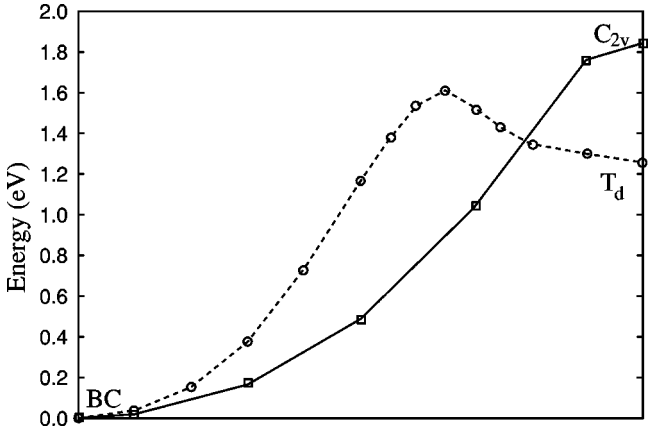

FIG. 2. Migration barrier for neutral bond-centered hydrogen. The full line and squares indicates the barrier to the C_{2v} saddle-point with *H* along the [001] direction, for hydrogen migrating directly between bond centers in a (110) plane. The dashed line and the circles show the barriers between the bond-centered interstitial (on the left) and the T interstitial (on the right).

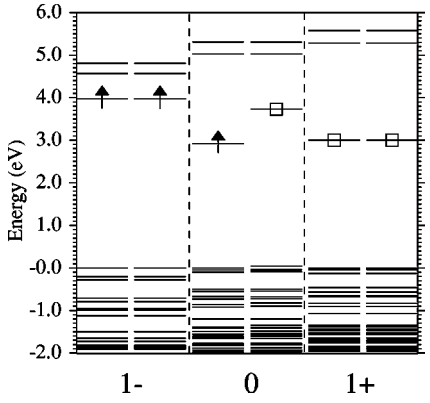

FIG. 3. The spin-polarized Kohn-Sham levels for the D_{3d} negatively, neutral, and C_{2h} positively charged bond-centered interstitial hydrogen. Only states in the vicinity of the band gap are plotted, and the valence-band tops have been aligned to facilitate comparison. The partially occupied gap level has a_{2u} symmetry.

The energies of the different configurations give a clue to the hydrogen diffusion path and energy barrier. The relatively high energy of H^0 at the *T* and *H* cage sites suggest that the H atom avoids these. This is in line with a previous study,[20] although other studies have suggested a BC to *T* site.[42] In silicon, similar calculations show the energy surface for neutral H to be very flat and a more elaborate process, involving jumps between next-nearest bond-centers via the *M* site (lying midway between two *C* sites) have been suggested.[56] It is unlikely that this mechanism operates in diamond as we find the *M* site to be unstable: a H atom placed there moves downhill in energy to reach a *T* site. The likely diffusion path then involves either a BC-*T*-BC or a BC-*C*-BC trajectory.

We estimated the migration barriers using cluster calculations by relaxing configurations intermediate to the beginning and end points of a diffusion jump, with constraints which prevent the structure relaxing into local minima. The barrier for hydrogen to move from a BC site to a *T* site is sketched in Fig. 2. Note that the energy for the *T* site is slightly higher than that listed in Table I derived from a supercell calculation, but the discrepancy is small. Also shown is an alternative trajectory for moving the H atom between BC sites in a (110) plane. The barrier for movement to the tetrahedral site is around 1.6 eV. Once H reaches this site, it can subsequently move to a number of bond centers, and hence diffuse through the lattice with this barrier. This barrier height is in agreement with earlier estimates.[20,42] The other path involving a direct BC to BC transition is activated with an energy of 1.8 eV (Fig. 2) with the saddle point found to be a C_{2v} structure with the hydrogen atom along the [001] direction. The diffusion through open channels, i.e., from a *T* site to another *T* site via the *H* site, has a barrier of 0.8 eV.

H_{BC} possesses a localized level deep in the band gap (Fig. 3). This level is associated with the highly dilated C-H-C bond (47% longer than the bulk bond length); for the D_{3d} case, the corresponding wave function possesses A_{2u} symmetry. One can estimate the location of the donor and acceptor levels by comparing its ionization energy and electron affinity, calculated in the cluster, with those of known defects.[6] Here we adopt the common terminology that the donor level is the value of the electron chemical potential below which the defect would be positively charged and above which it would be neutral. The acceptor level is defined in a similar way. Using the experimental $(0/+)$ level of *P* at $\sim E_c - 0.6$ eV as a marker, the cluster calculations yield the single donor level of BC hydrogen to lie around $E_c - 3$ eV. Note that this method for estimation of the electrical level uses entirely ground-state properties of each system.

The fact that H_{BC} is a deep donor has implications for any model involving hydrogen for a surface *p*-type conducting layer. Free hydrogen would be expected to compensate for any shallow acceptors, and since the overall concentration of hydrogen in the subsurface region is large (up to $\sim 10^{20}$ cm^{-3}), it cannot be present as an isolated hydrogen species.

In the negative charge state, unlike the case in silicon, the H atom still ''prefers'' to lie at the BC site. The gap level is now filled and the defect diamagnetic. There is no propensity for the defect to distort from D_{3d}. The barrier to migration in this charge state was also calculated. The BC to *T* and direct BC to BC paths have similar energies around 2 eV. Comparing the electron affinity of hydrogen with that of boron using the cluster method places the $(-/0)$ level of H_{BC} at $E_c - 1.8$ eV. The important conclusion is then that the acceptor level of H lies above the donor level, and thus hydrogen is a positive-*U* center in diamond. This is largely because the bond center, or one close to it, is the stable site for all charge states. The acceptor level lies below the $(0/+)$ level of P and is close to the donor level of N.

In the positive charge state, however, the proton moves off axis with a C-H-C bond angle around 100°, although the energy surface is very flat and relatively large changes in the bond angle do not greatly affect the total energy. This distortion from axial symmetry is accompanied by a drop of ~ 0.2 eV in energy. We have examined a number of different symmetries for this puckered bond-center configuration, and there appears to be no substantial difference in energy be-

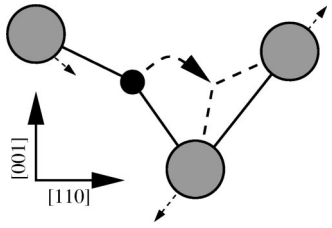

FIG. 4. A schematic representation of the rate-limiting step in the migration path for positively charged bond-centered hydrogen. The gray circles represent carbon sites in a $(1\bar{1}0)$ plane, and the black circle the hydrogen atom. The bond into which the H atom moves must dilate during the migration step.

tween different sites around the C-C bond. This suggests that in the positive charge state the proton precesses about the bond, giving a center with D_{3d} symmetry on average. Significantly the puckered configuration leads to a reduction in the dilation of the ''bond'' in which the hydrogen lies so that the distance between the carbon atoms is only 21% larger than in bulk. As a result the diffusion of H^+ is quite different from that in the other charge states. Figure 4 shows a trajectory taking the proton from a specific bond-center orientation to a different orientation in a second bond center. Since the barrier to precession is essentially zero, the proton can easily rotate into an equivalent site, thus completing a diffusive step. The barrier for this trajectory is estimated to be in the region of <0.2 eV when using constrained relaxation of a cluster: at least an order of magnitude lower than the diffusion barrier in the other charge states. The supercell approach yields a transition state (the *C* site) very close in energy to the puckered bond center (Table I). Hence H^+ is the most rapidly diffusing species, and its diffusion energy is not inconsistent with the experimental value of 0.35 eV found for deuterium introduced by a rf plasma as described above.

Besides the diffusion barriers, we have also calculated the local vibrational modes of these centers. Those lying above the Raman edge are listed in Table II. The defects possess C-H stretch modes lying between 2100 and 2900 cm^{-1}, corresponding to zero-point energies of 130–180 meV. Specifically examining the modes associated with the puckered structure in the positive charge state, one can see that the zero-point energy of the defect is of the order of the diffusive barrier. In a more complete analysis of the migration process one would therefore wish to consider quantum-mechanical tunneling. However, such a calculation is beyond the scope of this study, and we simply conclude that the migration of this center occurs at a very small barrier.

For each local mode we have also estimated the effective charges which govern the intensities of the absorption lines.[57] These are also listed in Table II. The values for the neutral and positive defects are very small in comparison to the value of $\sim 3e$ for H_{BC}^+ hydrogen in silicon,[7,54] but in line with the observation that C-H stretch modes for defects in Si generally have low integrated intensities.[58,59] With such small effective charges, it is possible that the defects are below the detection limit for infrared spectroscopy. The effective charge of H^- is much larger $\sim e$. However, as its diffusivity is so low, its penetration depth in say phosphorus or nitrogen doped diamonds would be expected to be much less.

IV. SOLUBILITY OF HYDROGEN IN DIAMOND

The equilibrium concentration of a hydrogen center in diamond is determined by its formation energy.[60,61] Interstitial hydrogen defects are formed through the addition of hydrogen atoms to the lattice, but substitutional or vacancy-hydrogen defects involve, in addition, the movement of carbon atoms to the surface. In either case, the formation energy of a single hydrogen defect in charge state q ($q>0$ for positively charged defects) is given by

$$E^f(\mathrm{H}^q) = E(\mathrm{H}^q + n\mathrm{C}) + q(E_v + \mu_e) - n\mu_\mathrm{C} - \mu_\mathrm{H}.$$

Here $E(\mathrm{H}^q + n\mathrm{C})$ is the total energy of the center evaluated in an n-atom unit cell. μ_C is the chemical potential of C, taken from the energy per C atom in bulk material. E_v is the position of the valence band top in the defect free crystal, and μ_e is the electron chemical potential measured from the valence-band top. μ_H is the chemical potential of hydrogen, taken with respect to a standard state. This can be a gas of molecular hydrogen outside diamond, although a gas of neutral hydrogen atoms can also be considered theoretically. Thus for equilibrium with a gas,[62,63]

$$\mu_\mathrm{H} = \frac{1}{2}E(\mathrm{H}_2) + \frac{kT}{2}\ln\left\{\left(\frac{p}{kT}\right)\left(\frac{\pi\hbar^2}{m_p kT}\right)^{3/2}\frac{1}{Z_{\mathrm{rot/vib}}}\right\}, \quad (1)$$

where the energy of a molecule is $E(\mathrm{H}_2)$, and includes the vibrational energy. $Z_{\mathrm{rot/vib}}$ is the partition function of the H_2 rotovibrator. In the case of equilibrium with a gas of isolated atoms,

$$\mu_\mathrm{H} = E(\mathrm{H}) + kT\ln\left\{\left(\frac{p}{kT}\right)\left(\frac{2\pi\hbar^2}{m_p kT}\right)^{3/2}\right\}, \quad (2)$$

where $E(\mathrm{H})$ is the energy of a neutral atom. The temperature-dependent term in each case can be ignored

TABLE II. Local vibrational mode frequencies and symmetries for bond-centered hydrogen in diamond (cm^{-1}). Frequencies for deuterium follow those for hydrogen (in parentheses). Also listed is the estimated value of η^2/m (e^2/amu). The modes for the positive charge state are taken from the C_{1h} form.

	1+			0			1−	
Mode	Symmetry	η^2/m	Mode	Symmetry	η^2/m	Mode	Symmetry	η^2/m
2456 (1797)	A'	2×10^{-3}	2919 (2084)	A_{2u}	1×10^{-4}	2730 (1952)	A_{2u}	1
2086 (1598)	A'	1×10^{-2}						

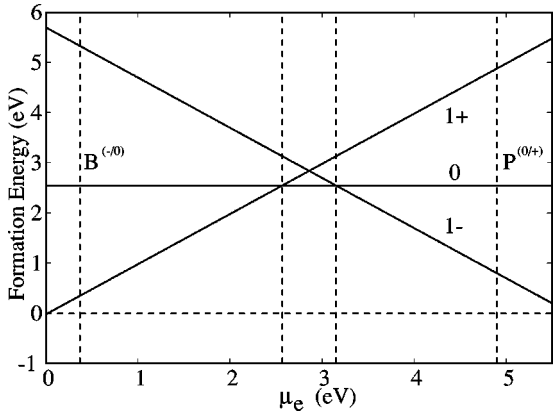

FIG. 5. Formation energies for the bond-centered H atom in the three charge states using the energy of the free H atom as chemical potential for hydrogen.

since, even for temperatures up to 1000 K, the contribution is less than 10%. For atmospheric pressure and $T=500$ K, the error in μ_{H} is 2.5% and 3.8% for molecular and atomic hydrogen, respectively. Note that the temperature-dependent part of μ_{H} tends to increase the formation energy with temperature.

A question arises as to whether these chemical potentials should be evaluated or taken from experiment. We have chosen to use the calculated potentials rather than their exact values, so that H is treated in the same way as within diamond and follows the procedure adopted by Van de Walle for H in silicon.[64] The energy of the neutral H atom evaluated in the supercell is -12.52 eV compared with the exact value of -13.61 eV, while the calculated binding energy of the free hydrogen molecule is 5.44 eV compared with an experimental value of 4.52 eV. The underestimate of the energy of atomic H is a well known, failing in local-density-functional theory, and the value found here compares with -13.03 eV given by Van de Walle.[64] These values determine μ_{H} relative to H_2 gas to be -15.24 eV when the contributions from vibrational and rotational degrees of freedom are excluded. These corrections amount to a few tenths of an eV, and to some extent are canceled by similar terms arising from the defects within diamond. The equilibrium concentration of H inside diamond is then given by

$$[\mathrm{H}]\sim N_s \exp\left(-\frac{E^f(\mathrm{H}^q)}{kT}\right),$$

where N_s is the number of sites the defect can occupy. A similar expression can be written down for the equilibrium concentration of hydrogen dimers.

The formation energies for H_{BC} are given in Table IV. It is clear that this energy of ~ 2.6–5 eV is very large, and as such neutral hydrogen is very insoluble in undoped diamond. We have checked the effect on formation energies using with wave function basis set. We find that, although the total energies vary significantly, the formation energies vary by only around 0.2 eV when using μ_{H} taken from the hydrogen molecule. The situation is less converged when using the value for μ_{H} taken from the isolated atom. Here $E^f(\mathrm{H}_{bc})$ ranges from 1.7 to 2.5 eV.

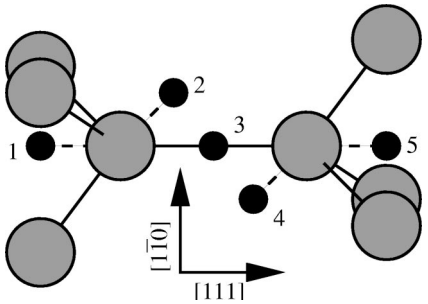

FIG. 6. Schematic showing H-atom sites for hydrogen dimers. Gray circles represent carbon sites, and black circles numbered 1–5 show possible sites for hydrogen.

The formation energy is also dependent on the charge state. Figure 5 shows its variation with Fermi energy. In this case, we have taken μ_{H} to be given by the free atom, but a similar plot with μ_{H} taken from the free molecule simply adds around 2.5 eV to the energies. Such a plot allows the energy levels for hydrogen to be estimated. The $(0/+)$ level occurs at a Fermi energy where the formation energies of the neutral and positive charge states are equal. This lies around $E_v+2.6$ eV. Similarly, the acceptor level is found around $E_c-2.3$ eV. Both estimates are in agreement with the values found in the cluster calculations.

Also plotted in Fig. 5 are the experimental locations of the acceptor level of boron ($E_v+0.37$ eV) (Ref. 65) and the donor level assigned for substitutional phosphorus ($E_c-0.6$ eV).[66] From these, one concludes that the formation energy for H^+ in strongly *p*-type material is about 0.3–0.4 eV, implying an equilibrium solubility at 500 °C of the order of that seen in the subsurface region in plasma treated material. The formation energy of H^- in strongly *n*-type material is ~ 1 eV. However, when the H concentration is comparable with that of boron or phosphorus, the Fermi energy must move close to mid-gap and the equilibrium concentration of neutral H becomes essentially zero. Thus the maximum equilibrium concentration is pinned by the acceptor-donor concentration. However, the state of hydrogen in pure, boron-doped or nitrogen-doped diamond need not be the isolated hydrogen defect. There is a possibility that it is more stable as a dimer or impurity-hydrogen pair and these are investigated below. Note that including temperature effects in Eqs. (1) and (2) would lead to higher formation energies than those listed in Table IV and shown in Fig. 5. This would only affect the properties of potentially soluble species such as the positive charge state in heavily boron-doped material.

V. HYDROGEN DIMERS

A possibility alluded to above is that hydrogen dissolved in the material is in the form of self-trapped hydrogen complexes. We have examined a number of possible structures based on those suggested to exist in silicon. These are an interstitial hydrogen molecule which is the lowest energy structure for silicon, H_2^* (sites 1 and 3 in Fig. 6), previously[19,20] found to be the lowest energy structure in diamond, a pair of antibonded hydrogen atoms along $\langle 111\rangle$

TABLE III. Relative total energies of the interstitial H pairs in diamond (eV). The zero for the energy scale for each charge state is taken to be the energy of the most stable structure examined in this study, *viz.*, H_2^*.

	H_2^*	H_{2BC}	H_2^{**}	Molecule
Neutral	0.0	0.8	1.9	2.1
1+	0.0	0.0	1.3	1.2

labeled H_2^{**} (sites 1 and 5 in Fig. 6), and a pair of hydrogen atoms saturating a single broken C-C bond with C_{2h} symmetry (H_{2BC}, sites 2 and 4, Fig. 6).

The total energies of these defects evaluated in a 64-atom unit cell are listed in Table III. As found by previous *ab initio* calculations, both cluster and supercell methods yield H_2^* as the most stable dimer; in particular, it is 2.1 eV lower in energy than the molecule at the T_d interstitial site when using the supercell. The Kohn-Sham levels (Fig. 7) indicate that the defects might be electrically active, although the calculated donor level lies very close to E_v. The gap levels are mainly localized on C-H bonds and the neighboring perturbed C-C bonds. In the positive charge state, H_{2BC} and H_2^* defects are comparable in energy.

The vibrational modes of H_2^* lie at 3511 and 3882 cm^{-1} (A_1) and 1782 cm^{-1} (E). However, like H_{BC}, the effective charge for each mode is small ($\eta^2/m < 2\times10^{-2}e^2$). Thus the defect is electrically inert, diamagnetic, and optically inactive, making its detection exceptionally difficult. It might then be part of the accumulation layer introduced by rf plasmas.

The binding energy of the H atoms in H_2^*, found by comparing the energies of two isolated H_{BC} atoms with the complex, is around 2.5 eV. Its diffusion mechanism involves a partial dissociation into two BC-sited H atoms separated by a C-C bond, and can proceed in two consecutive but equivalent steps, as illustrated in Fig. 8. The first step (labeled 1 in the figure) moves the antibonding species into a bond center.

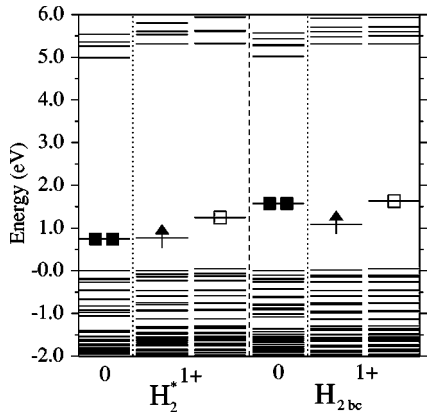

FIG. 7. The Kohn-Sham levels for the neutral (spin averaged) and positively charged (spin-polarized) H_2^* and H_{2bc} defects. Only states in the vicinity of the band gap are plotted, and the valence-band tops have been aligned to facilitate comparison. Black squares and arrows represent filled levels, and empty squares indicate unoccupied levels.

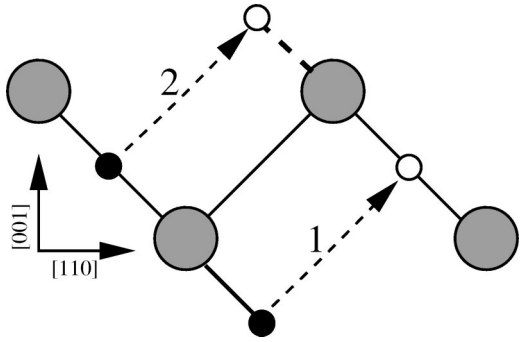

FIG. 8. Schematic of a diffusion path for H_2^*, as described in the text. Processes 1 and 2 are sequential, not simultaneous. The large gray circles represent C atoms in a $(1\bar{1}0)$ plane. The small black and white circles represent the start and end positions, respectively, for the hydrogen atoms.

The second step is then the reverse of this process where the second H atom (labeled 2 in Fig. 8) jumps to reform H_2^* displaced by one atomic site from the original site. The activation energy exceeds 3.5 eV, and is greater than the binding energy. This large value implies that H_2^* would be immobile at temperatures less than about 1000 °C.

In contrast with H_2^*, the molecule diffuses relatively freely with a barrier of about 1.6 eV between the T and H sites. This energy is close to the diffusion energy of H_{BC} in the neutral and negative charge states.

The formation energies of the dimers are given in Table IV. Again, these values are large and positive, showing that the equilibrium concentrations of these defects will be insignificant. In summary, H_2^* is the most stable dimer but its equilibrium concentration is negligible. It is nonmagnetic and electrically and optically inert. It is a candidate for the hydrogen defects in the accumulation layer possibly introduced by the channeling of hydrogen ions from the plasma.[67] These ions will be accelerated if the diamond is biased. However, this process is also likely to create lattice damage which might lead to other types of hydrogen species such as hydrogen trapped at dislocations.

VI. BORON-HYDROGEN COMPLEXES

Since the only unambiguous assignment of a point defect in bulk diamond which contains hydrogen is that of the boron-hydrogen pair, we have investigated this defect in detail. The formation energy of substitutional boron can be obtained using the same approach as adopted for hydrogen (Sec. IV), where now a carbon atom is replaced by boron. We suppose the chemical potential of boron is determined by

TABLE IV. Formation energies per hydrogen atom (eV) for the neutral bond-centered H atom and two configurations of the H dimer, for which we list the chemical potential in parentheses.

Reference state of H	H_{BC}	H_2^*	Molecule
H atom (−0.92 Ry)	2.6	1.0	2.1
H_2 (−1.12 Ry)	5.2	3.7	4.8

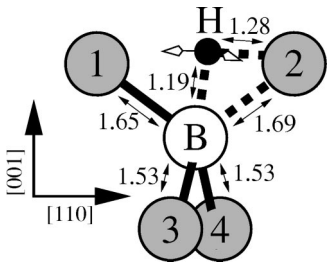

FIG. 9. Schematic diagram for the structure of the boron-hydrogen pair in diamond. Gray circles represent carbon atoms. The white arrows indicate one of localized modes of vibration as described in the text. The bond lengths are shown in Å.

BH_3. In this case $\mu_B^{BH_3}=E(BH_3)-\frac{3}{2}E(H_2)$. The formation energy for B in diamond is calculated to be close to zero, broadly consistent with the high doping levels of $\sim 10^{22}$ cm^{-3} achievable in polycrystalline CVD material.

We now discuss the hydrogenated center. As with earlier *ab initio* calculations, we found that the structure where H lies approximately along the [001] direction from the B atom was most stable (Fig. 9). The total energy is 0.6 eV lower than when H lies in the C-B bond center.

The binding energy of the complex can be estimated both for the case of dissociation into neutral boron and bond-centered hydrogen, and for the case where the products are charged as in H^+ and B^-, i.e.,

$$E^b(BH)=E^f(B)+E^f(H)-E^f(BH)$$

or

$$E^b(BH)=E^f(B^-)+E^f(H^+)-E^f(BH),$$

where $E^f(X)$ is the formation of X as defined above. The results are 4.0 and 1.6 eV, respectively, indicating, as expected, that dissociation of the pairs produces H^+ and B^-. The dissociation barrier is estimated to be 1.8 eV by moving H to a bond-center neighboring B. This is in good agreement with the activation energy for the diffusion of H found in samples exposed to a microwave plasma where the H concentration is close to that of B.

The vibrational modes of the complex have also been calculated (Table V). There are two modes at 2664 and 1975 cm^{-1}. The lower is a wag mode lying in the plane of symmetry of the defect, and is much higher in energy than the barrier to the equivalent site for the H atom in this plane. In practice the system is likely to tunnel between equivalent σ_H sites yielding an effectively C_{2v} defect. The effective charge for the higher frequency mode is estimated to lie around $0.1e$ for an oscillator with unit mass.

Figure 10 shows the charge density in the neighborhood

TABLE V. Local vibrational modes of the B-H pair in diamond (cm^{-1}) for the various isotope combinations.

^{10}BH	^{11}BH	^{10}BD	^{11}BD
2664	2654	1973	1956
1975	1971	1530	1525

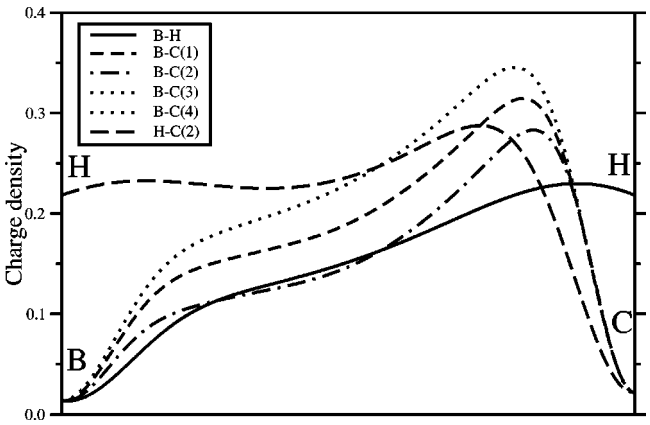

FIG. 10. A plot of the charge density between the B atom and its five neighbors as a function of position along the bond. The labeling follows Fig. 9. Note that the small values at the B and C sites are a consequence of the use of pseudopotentials. All bonds are scaled to the same internuclear distance.

of boron, hydrogen, and carbon (as labeled in Fig. 9). The low charge density shows that the B-C(2) bond is weaker than the others due to the presence of the hydrogen atom, but still has a bonding character. More significantly, the H-C(2) bond indicated by the long-dashed line contains a greater charge density than between the boron and hydrogen (solid line). There appears to be a tendency to form a multicentered B-H-C(2) bond which is typical of bond hydrides, e.g., diborane (B_2H_6) in which two BH_4 tetrahedra share an edge.

It is worth noting that boron conventionally ''prefers'' threefold coordination, i.e., a breaking of the B-C(2) bond, leaving H to passivate C(2). Figure 10 shows that the B-C(2) bond is the weakest and that the H-C(2) bond is far stronger than the B-H bond. Qualitatively, one can consider this system to arise from a linear combination of the several bonding patterns, one of which is the threefold-coordinated B. One then includes conventional sp^3 hybrid of B_s with H antibonding. A further contribution arises from the average C_{2v} structure [H midway between C(1) and C(2)], where boron is sp^2 hybridized, with conventional pair bonds to H, C(3), and C(4). An unhybridized B p orbital (along the $\langle 110\rangle$ direction) then forms a multicentered bond with sp^3 hybrids on C(1) and C(2).

The Kohn-Sham levels of the complex (Fig. 11) indicate that there are no deep states in the gap, and hence that the boron has been passivated by the addition of the H atom.

VII. DONOR-HYDROGEN COMPLEXES

The formation energy of the single substitutional N defect can be found as described above when μ_N is determined by a gas of N_2 molecules. This gives a value close to zero, consistent with the observed high solubility of nitrogen in diamond, although the precise value of the formation energy varies with basis set. Then one would expect that diamonds grown in the presence of nitrogen and hydrogen, such as is the case for polycrystalline material, nitrogen-hydrogen complexes will be present in the material. It is known that CVD samples also exhibit sharp IR-absorption lines associated

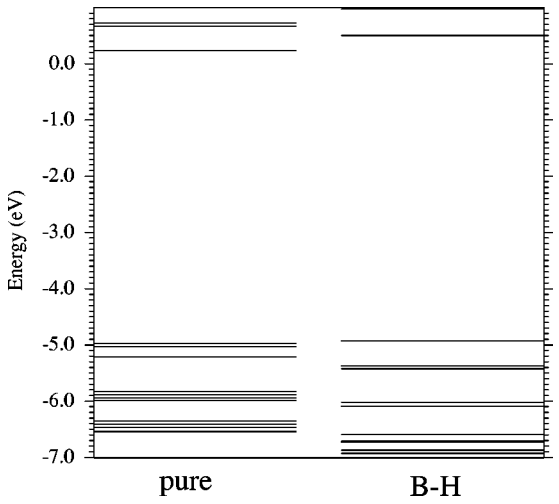

FIG. 11. The Kohn-Sham levels for a pure diamond cluster and one containing a B-H complex. Only levels in the vicinity of be band gap are plotted. No gap states are present for the B-H complex. All levels below around -4.9 eV are filled, and all other levels are empty.

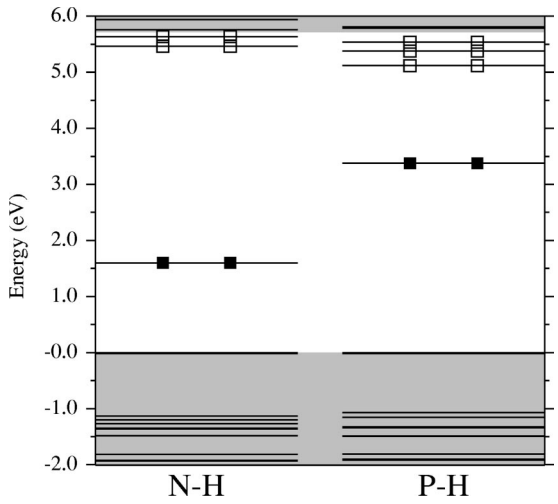

FIG. 12. The Kohn-Sham levels of N-H and P-H complexes. Only levels in the vicinity of be band gap are plotted. The gray shaded areas correspond to valence and conduction bands for the pure diamond unit cell. The valence bands are aligned to zero.

with hydrogen that exhibit the same ^{13}C shift as the 3107 cm^{-1} band seen in natural material, but with frequencies shifted upward by $\sim$17 cm^{-1}.[23]

The structures and binding of hydrogen to N and P were found using 64-atom cubic unit cells. We investigated four sites for the donor-hydrogen pairs. These are (a) bond centered, (b) antibonding to the donor, (c) antibonding to a C neighbor to the donor, and (d) a configuration similar to that found above for the boron-hydrogen complex where the hydrogen atom lies approximately along the [001] direction from the donor impurity.

In the case of nitrogen, structure (a) in which H is located near a bond center between N and C was the most stable. Structure (d) was unstable and relaxed to (a). Structures (c) and (b) were less stable than (a) by 1.4 and 3.0 eV, respectively. In the stable structure (a), the H-C and H-N bond lengths are 1.06 and 1.26 Å, respectively, and agree with earlier semiempirical calculations.[43] Figure 12 shows its Kohn-Sham eigenvalues. These suggest that the complex possesses a deep donor level in the lower half of the band gap, and thus N is not completely passivated by H, i.e., this complex is potentially a deep donor. We estimate the $(0/+)$ level of N...H-C to lie around $E_v+1.1$ eV compared to the experimental level of substitutional nitrogen at $E_c-1.7$ eV. However, since these centers would necessarily only exist in large concentrations in material which contains a high density of substitutional N atoms, the electron chemical potential is unlikely to lie sufficiently low in the gap to ionize the center. The presence of an empty Kohn-Sham level just below the conduction-band minimum is not considered to be significant, since there is some uncertainty in the actual location of the band edge.

The defect can dissociate into neutral or charged species and we find binding energies of 3.5 and 4.2 eV, respectively, for the two cases. These are much larger than the 1.49 eV found by another method.[43] The relatively small difference between the binding energies of the neutral and charged defects contrasts with B-H, and reflects the proximity of the hydrogen acceptor level to the nitrogen donor level. The large binding energy will lower the formation energy of H and increase its solubility. Figure 5 shows that the formation energy of H is then about -1 eV for a gas of free H atoms, and about 1.5 eV using μ_{H} derived from molecular hydrogen. Thus, in polycrystalline CVD material, the presence of N will encourage the incorporation of hydrogen and the formation of N...H-C defects. Once formed, the large binding energy implies a very stable defect.

We have calculated the deep donor level of the N...H-C center by comparing the formation energies of the neutral and charged states. This leads to a donor level around $E_v+1.5$ eV. The defect does not possess an acceptor level.

A high-frequency stretch mode lies at 3324 cm^{-1}, which shifts by 6 and 910 cm^{-1} with ^{13}C and deuterium, respectively. Both shifts are smaller than one would expect for harmonic oscillators, indicating the importance of anharmonicity. This is known to be significant for other C-H stretch modes.[68] Of great interest is that the isotopic shift due to ^{15}N is very small and <0.1 cm^{-1}. The H-related bend mode of *E*-mode symmetry lies at 1400 cm^{-1}, and drops below the Raman to around 972 cm^{-1} in the case of deuterium. The 1400-cm^{-1} mode shifts by less than 0.5 cm^{-1} when the nearest neighbors are set to ^{13}C or ^{15}N.

It is tempting to assign the commonly occurring 3107-cm^{-1} band with the defect. Previously the involvement of nitrogen in the 3107-cm^{-1} band was excluded because of the absence of a shift with ^{15}N, but our results show that the shift is very small. Overtones of the 3107-cm^{-1} band have been observed[22] and, while the symmetry of the defect remains unknown, they demonstrate that the center, like the N...H-C defect, does not possess inversion symmetry. In ^{13}C material, the 3107-cm^{-1} band shifts about 9 cm^{-1}, in fair agreement with the calculated shift of 6 cm^{-1}. No deuterium-related modes around 2256 cm^{-1} were found for

the defect. It may be that they possess a very short lifetime due to decay into two optical phonons.[23] The calculated effective charge of the N...H-C stretch mode is of the order of $1e$, and very large in comparison with neutral bond-centered interstitial hydrogen.

Our calculated stretch mode is around 7% higher than the 3107-cm^{-1} band. As a rule of thumb, a 3% error in bond length would be expected to give rise to a 10% error in stretch mode frequency. For C-H complexes in GaAs, the method employed for this study is known to overestimate the stretch mode by around 10%. Therefore, we conclude that the calculated local modes are consistent with an assignment of the 3107-cm^{-1} band to the N...H-C defect. It is interesting to note that although the 3107-cm^{-1} band is seen in a variety of materials, it is always seen in nitrogen-rich type-Ib pure diamond, and rarely observed in type-IIa pure diamonds.[24,69,25] In summary, the strong binding energy between N and H will increase the solubility of H in nitrogen-doped diamond. The N...H-C defect has a deep donor level and a H-related stretch mode with isotopic shifts consistent with the commonly detected 3107-cm^{-1} mode. However, the calculations are also consistent with the similar band seen in CVD material at 3124 cm^{-1},[23] and it is impossible to distinguish between them from our results.

We now investigate the influence of H on the phosphorus donor. The structure of the phosphorus-hydrogen defect is quite different from the nitrogen center. Structure (b), where H antibonds to the P atom, is the most stable. Structures (a), (c), and (d) are 3.5, 1.7, and 1.5 eV higher in energy, respectively.

The P-H bond is 1.34 Å, and the three equivalent P-C bonds are 1.70 Å, while the axial P-C bond is 1.75 Å. The electronic properties of the defect resembles that of the N...H-C defect above. Although the Kohn-Sham levels shown in Fig. 12 reveal a number of empty gap states close to the conduction band, the defect only possesses a donor level around $E_c - 3.0$ eV.

The H and D stretch modes lie at 2985 and 2142 cm^{-1}, respectively, although these values are probably overestimated. The H- and D-related bend modes are calculated to be 2016 and 1537 cm^{-1}, respectively. The estimated effective charges for the P-H stretch and bend modes are both $\sim 0.1e$, and therefore should be detectable. The binding energy for dissociation into neutral or charge components are 3.1 and 1.0 eV, respectively. This suggests that, unlike the N...H-C defect, the complex is stable only to relatively low temperatures.

As with the other impurities, we have estimated the formation energy for neutral substitutional phosphorus. Taking μ_P from phosphene (PH_3) gives formation an energy $E^f(P_s)$ equal to 7.2 eV. It seems clear that the equilibrium solubility of P in diamond is very low indeed. Its incorporation from PH_3 in polycrystalline CVD diamond must then be a consequence of kinetic factors possibly linked to hydrogen. One possibility is that P-H itself has a low formation energy, and that the hydrogen can be removed by a post-growth anneal. Therefore an important quantity is the relative formation energies of P-H and substitutional P:

$$E^f(\mathrm{PH}) - E^f(\mathrm{P}) = E^f(\mathrm{H}) - E^b(\mathrm{PH}).$$

From Fig. 5, we see that this quantity is close to zero for a Fermi-energy locked to the P donor level. Thus, although the equilibrium concentrations of P-H and P defects are comparable, the solubility of P-H is not significantly greater than P. Hydrogen does not then increase the solubility of P, but rather the solubility of H is increased by P. This suggests that, unlike other systems such as Mg in GaN (Ref. 70) and C in GaAs,[71] a significant increase in the population of passivated dopant atoms does not occur for a vapor-phase-containing atomic hydrogen and phosphorus. Co-doping then does not seem to be favored, although it is recognized that other mechanisms might operate and lead to a large phosphorus incorporation. For example, atomic hydrogen might modify the surface of the diamond which leads to a greater incorporation of phosporus.

VIII. HYDROGEN IN A STRAIGHT DISLOCATION

A question arises as to the structure of hydrogen in the subsurface reservoir introduced by a rf plasma. One possibility is that this is in the form of H_2^*, which, as explained above, would be very difficult to detect by infrared-absorption experiments, although channeling remains a possibility. The high concentration appears to exclude grain boundaries, and we have examined the possibility that the hydrogen is trapped at a dislocation. Dislocations are present in all types of diamonds and, in silicon, it is known that they can trap hydrogen.[72,73]

In Si and diamond, the commonly occurring 60° and screw dislocations lie on {111} planes and are dissociated into 90° and 30° partials separated by an intrinsic stacking fault. The dissociation reaction is

$$\frac{a}{2}[1\bar{1}0] \rightarrow \frac{a}{6}[1\bar{2}\bar{1}] + \frac{a}{6}[2\bar{1}\bar{1}].$$

We investigate only the 90° partial here. Earlier calculations[74] indicated that all the bonds in this partial are reconstructed with a dilated C-C bond of length 1.61 Å across the core. More recent work suggested that the core is more complicated and has periodicity twice that shown in Fig. 13.[75] Nevertheless, all bonds are again reconstructed suggesting that the effect of hydrogen on both forms will be similar.

The binding energy for a single H atom to the core is found to be about 1.9 eV. However, it is to be expected that its diffusion barrier along the core will be comparable with bulk diffusion, with an activation barrier calculated to be 1.2 eV.[76] Thus if it is able to diffuse to the core, then it will also be able to diffuse along the core possibly leading to the creation of hydrogen dimers. The most stable dimer found at the core is H_{2BC} (sites 2 and 4 in Fig. 6) and 1.7 eV more stable than H_2^*. The energy difference between H_{2BC} at the core and an isolated H_2^* defect is -4.0 eV, showing that H_2^* is unstable in the presence of dislocations. The stability of H_{2BC} at the core is a consequence of the dilated C-C bond there, and thus the defect is expected to be stabilized by any dislo-

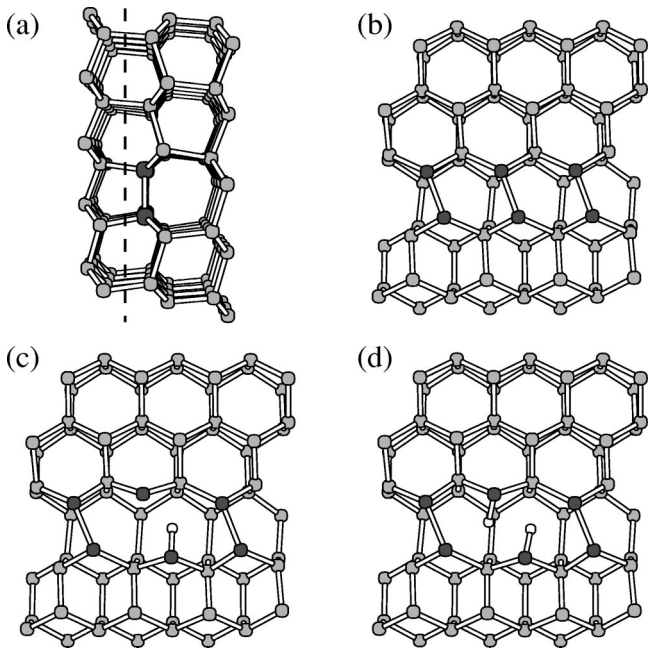

FIG. 13. Schematics for the dislocation structures investigated. (a) The relaxed dislocation core viewed down the dislocation line. (b)–(d) Sections of dislocation where material to the left of the dashed line in (a) is removed for clarity. (b) The undecorated disloaction; the three reconstructed bonds are indicated by the dark atoms. (c) and (d) Relaxed structures for the single hydrogen trapped at the core and H_{2BC}, respectively, where the hydrogen is indicated by white atoms.

cation or dilated bonds at grain boundaries. The large binding energy of hydrogen with the dislocation is largely due to the breaking of the weakened core C-C bonds and the relaxation of strain. A possibility, suggested by Heggie *et al.*,[76] is that dislocations are spontaneously formed in the presence of hydrogen and the subsurface accumulation layer arising from rf plasmas readily explained.

The local vibrational modes of the H_{2BC} defect at the dislocation core are found to be 1458, 1787, 3718, and 3775 cm^{-1}. Their effective charges are calculated lie between 0.1 and 0.5*e* for a unit mass. Since the whole dislocation line is likely to be hydrogenated, the coupling between modes leads to broadened bands but only the tranverse optic modes at the zone center can be infrared active. These frequencies seem too high to correspond to the 3107-cm^{-1} mode seen experimentally, but it is possible that another configuration of hydrogen at an extended defect is responsible for this absorption.

Estimates of the dislocation density are difficult to make, and are very variable, but values up to 10^{12} cm^{-2} were suggested as an upper limit.[77] This would imply a maximum concentration of core hydrogen of the order of 10^{20} cm^{-3}. This hydrogen concentration is comparable to that of boron[33] around 5×10^{19} cm^{-3}, but considerably less than the peak subsurface concentration of 10^{22} cm^{-3} found in the rf plasma treatment. Unless dislocations are created by the presence of high concentrations of H (concomitant with the condensation of H suggested in Ref. 76), additional hydrogen defects must be present with H_2^* as one candidate.

IX. CONCLUSION

Calculations have shown that hydrogen, when incorporated in bulk diamond, is expected to form bond-centered hydrogen defects, stable H_2^* defects, B-H, N-H, and P-H centers, and be strongly trapped at dislocation cores. These are similar properties to hydrogen in silicon.

In contrast to H in silicon and many other materials, isolated hydrogen in diamond is not a negative-*U* center. This is due to the fact that hydrogen lies in the bond-centered site in all three charge states.

The calculated formation energies provide a semiquantitative estimate of the solubility of hydrogen in diamond. The large positive values for isolated and hydrogen dimers suggest that the equilibrium solubility for hydrogen in the lowest energy states we have found is vanishingly small. However, the large binding energy associated with hydrogen at impurities, lattice damage or in regions of strained material such as at dislocations or grain boundaries means that hydrogen would readily precipitate at these defects.

Unlike silicon, it is only the positively charged bond-centered species that is particularly mobile and if present in the material is likely to be quickly lost to defects or the surface. This species may be the fast diffusing one found using radio frequency plasmas.[32] There the subsurface deuterium concentration exceeds that of boron, allowing D^+ to diffuse freely to unpassivated boron lying deeper in the sample.

Neutral bond-centered hydrogen has a local mode with a very small effective charge implying that it would be invisible to IR spectroscopy, but this defect should be observable via EPR. The negatively charged defect has a greater effective charge, and hence should be IR active, but its diffusivity is much lower suggesting that it may not penetrate deeply into diamond.

Hydrogen dimers such as the diamagnetic and weakly IR-active H_2^* center are stable, and may account for the large concentrations of hydrogen found in many diamonds. This defect is more stable than molecular hydrogen in contrast with the situation in silicon.

Boron-hydrogen complexes have binding energies of around 1.6 eV, and appear to limit the diffusivity of hydrogen in type-IIb diamond. This is similar to the case in boron-doped Si, and is in agreement with diffusion experiments carried out with microwave plasmas and boron-doped polycrystalline CVD diamond.[33] The structure of the defect is quite distinct from silicon where the H atom bonds closely to the boron atom and lies in the bond center. The H atom is located almost midway between two C atoms and the local modes of B-H are likely to be complex due to the tunneling of the hydrogen between equivalent sites around the impurity.

In analogy to boron, we find that both N and P are essentially passivated by hydrogen, although the complexes possess donor levels close to the valence-band top. The structure and vibrational modes of N…C-H are consistent with the observed properties of the defect giving rise to the 3107- and/or 3124-cm^{-1} absorption bands. Hydrogen antibonds to phosphorus, giving characteristic local modes. The binding

energy of H with the donors is too low to offset the large positive formation energies of hydrogen defects. If the addition of PH_3 to the seed gases used in CVD diamond growth leads to a significant donor concentration, then it is likely that its incorporation is due to a surface effect.

Finally, we find that hydrogen strongly interacts with dislocation cores, breaking the core reconstruction and forming C-H defects. The binding energy of H_2^* with the core is around 4 eV, implying that this is a particularly stable form of hydrogen likely to be present in all types of diamond. This form of hydrogen, together with H_2^* may account for the subsurface accumulation layer detected when radio frequency plasmas are used to incorporate hydrogen.

ACKNOWLEDGMENTS

We acknowledge supercomputing support from EPSRC under the e6 (*Ab initio* simulation of covalent materials) consortium. M.I.H. and C.P.E. acknowledge the Sussex High Performance Computing Initiative and EU InterregII project: Transdiam.

[1] Y.V. Gorelkinskii and N.N. Nevinnyi, Physica B **170**, 155 (1991).
[2] B. Bech Nielsen, K. Bonde Nielsen, and J.R. Byerger, Mater. Sci. Forum **143–147**, 909 (1994).
[3] K. Bonde Nielsen, B. Bech Nielsen, J. Hansen, E. Andersen, and J.U. Andersen, Phys. Rev. B **60**, 1716 (1999).
[4] C.G. Van de Walle and P.E. Blochl, Phys. Rev. B **47**, 4244 (1993).
[5] K. Bonde Nielsen, I. Dobaczewshi, S. Søgård, and B. Bech Nielsen (private communication).
[6] A. Resende, R. Jones, S. Öberg, and P.R. Briddon, Phys. Rev. Lett. **82**, 2111 (1999).
[7] M. Budde, Ph.D. thesis, Aarhus Center for Atomic Physics, University of Aarhus, Denmark, 1998.
[8] A. Van Weiringen and N. Warmholz, Physica (Amsterdam) **22**, 849 (1956).
[9] A. Mainwood and A.M. Stoneham, Physica B & C **116**, 101 (1983).
[10] K.J. Chang and D.J. Chadi, Phys. Rev. Lett. **62**, 937 (1989).
[11] R.E. Pritchard, M.J. Ashwin, J.H. Tucker, and R.C. Newman, Phys. Rev. B **57**, 15 048 (1998).
[12] J.D. Holbech, B. Bech Nielsen, R. Jones, P. Sitch, and S. Öberg, Phys. Rev. Lett. **71**, 875 (1993).
[13] M.J. Binns, S.A. McQuaid, R.C. Newman, and E.C. Lightowlers, Semicond. Sci. Technol. **8**, 1908 (1993).
[14] B. Bech Nielsen, L. Hoffmann, M. Budde, R. Jones, J. Goss, and S. Öberg, Mater. Sci. Forum **196–201**, 933 (1995).
[15] M. Budde, B. Bech Nielsen, P. Leary, J. Goss, R. Jones, P.R. Briddon, S. Öberg, and S.J. Breuer, Phys. Rev. B **57**, 4397 (1998).
[16] E. Holzschuh, W. Kündig, P.F. Meier, B.D. Patterson, J.P.F. Sellschop, M.C. Stemmet, and H. Appel, Phys. Rev. A **25**, 1272 (1982).
[17] T.A. Claxton, A. Evans, and M.C.R. Symons, J. Chem. Soc., Faraday Trans. **82**, 2031 (1986).
[18] T.L. Estle, S. Estreicher, and D.S. Marynick, Phys. Rev. Lett. **58**, 1547 (1987).
[19] P.R. Briddon, R. Jones, and G.M.S. Lister, J. Phys. C **21**, L1027 (1988).
[20] S.P. Mehandru and A.B. Anderson, J. Mater. Res. **7**, 689 (1992).
[21] D. Saada, J. Adler, and R. Kalish, Phys. Rev. B **61**, 10 711 (2000).
[22] G. Davies, A.T. Collins, and P. Spear, Solid State Commun. **49**, 433 (1984).
[23] F. Fuchs, C. Wild, K. Schwarz, W. Müller-Sebert, and P. Koidl, Appl. Phys. Lett. **66**, 177 (1995).
[24] W.A. Runciman and T. Carter, Solid State Commun. **9**, 315 (1971).
[25] E.A. Burgemeister and M. Seal, Nature (London) **279**, 785 (1979).
[26] J. P. F. Sellschop, H. J. Annegarn, C. Madiba, R. J. Keddy, and M. J. Renan, Ind. Diamond Rev. Suppl. 2–4 (1977).
[27] B. Dischler, C. Wild, W. Müller-Sebert, and P. Koidl, Physica B **185**, 217 (1993).
[28] M. Seal, Nature (London) **212**, 1528 (1966).
[29] X. Zhou, G.D. Watkins, Rutledge. K.M. McNamara, R.P. Messmer, and S. Chawla, Phys. Rev. B **54**, 7881 (1996).
[30] D.F. Talbot-Ponsonby, M.E. Newton, J.M. Baker, G.A. Scarsbrook, R.S. Sussmann, A.J. Whitehead, and S. Pfenninger, Phys. Rev. B **57**, 2264 (1998).
[31] D. Ballutaud, F. Jomard, Duigou. J. Le, B. Theys, J. Chevallier, A. Deneuville, and F. Pruvost, Diamond Relat. Mater. **9**, 1171 (2000).
[32] J. Chevallier, D. Ballutaud, B. Theys, F. abd. Deneuville. A. Jomard, E. Gheeraert, and F. Pruvost, Phys. Status Solidi A **174**, 73 (1999).
[33] J. Chevallier, B. Theys, A. Lusson, C. Grattepain, A. Deneuville, and E. Gheeraert, Phys. Rev. B **58**, 7966 (1998).
[34] R.R. Zeisel, C.E.C.E. Nebel, and M. Stutzmann, Appl. Phys. Lett. **74**, 1875 (1999).
[35] H.J. Looi, R.B. Jackman, and J.S. Foord, Appl. Phys. Lett. **72**, 353 (1998).
[36] K. Hayashi, S. Yamanaka, H. Watanabe, T. Sekiguchi, H. Okushi, and K. Kajimura, J. Appl. Phys. **81**, 744 (1997).
[37] K. Hayashi, S. Yamanaka, H. Okushi, and K. Kajimura, Appl. Phys. Lett. **68**, 376 (1996).
[38] S.G. Ri, T. Mizumasa, Y. Akiba, Y. Hirose, T. Kurosu, and M. Iida, Jpn. J. Appl. Phys. **34**, 5550 (1995).
[39] J. Ristein, F. Maier, M. Riedel, M. Stammer, and L. Ley, Diamond Relat. Mater. **10**, 416 (2001).
[40] J.P. Goss, B. Hourahine, R. Jones, M.I. Heggie, and P.R. Briddon, J. Phys.: Condens. Matter **13**, 8973 (2001).
[41] B.P. Doyle, R.D. Maclear, S.H. Connell, P. Formenti, I.Z. Machi, J.E. Butler, P. Schaaff, J.P.F. Sellschop, E. SiderasHaddad, and K. Bharuth-Ram, Nucl. Instrum. Methods Phys. Res. B **130**, 204 (1997).
[42] M. Kaukonen, J. Peräjoki, R.M. Nieminen, G. Jungnickel, and Th. Frauenheim, Phys. Rev. B **61**, 980 (2000).
[43] S.P. Mehandru and A.B. Anderson, J. Mater. Res. **9**, 383 (1994).
[44] S.J. Breuer and P.R. Briddon, Phys. Rev. B **49**, 10 332 (1994).

[45] R. Jones and P. R. Briddon, in *Identification of Defects in Semiconductors*, edited by M. Stavola, Vol. 51A Semiconductors and Semimetals (Academic Press, Boston, 1998), Chap. 6.
[46] J. Coutinho, R. Jones, P.R. Briddon, and S. Öberg, Phys. Rev. B **62**, 10 824 (2000).
[47] R. Jones, P.R. Briddon, and S. Öberg, Philos. Mag. Lett. **66**, 67 (1992).
[48] J.P. Goss, R. Jones, S.J. Breuer, P.R. Briddon, and S. Öberg, Phys. Rev. Lett. **77**, 3041 (1996).
[49] B.J. Coomer, A. Resende, J.P. Goss, R. Jones, S. Öberg, and P.R. Briddon, Physica B **273–274**, 520 (1999).
[50] J.P. Goss, B.J. Coomer, R. Jones, T.D. Shaw, P.R. Briddon, M. Rayson, and S. Öberg, Phys. Rev. B **63**, 195208 (2001).
[51] G.B. Bachelet, D.R. Hamann, and M. Schlüter, Phys. Rev. B **26**, 4199 (1982).
[52] D. Liberman, Phys. Rev. B **62**, 6851 (2000).
[53] B. Clerjaud and D. Côte, J. Phys.: Condens. Matter **4**, 9919 (1992).
[54] B. Bech Nielsen, K. Tanderup, M. Budde, K. Bonde Nielsen, J.L. Lindstrom, R. Jones, S. Öberg, B. Hourahine, and P.R. Briddon, Mater. Sci. Forum **258–263**, 391 (1997).
[55] B. Hourahine (private comunication).
[56] C.G. Van de Walle, P.J.H. Denteneer, Y. Bar-Yam, and S.T. Pantelides, Phys. Rev. B **39**, 10 791 (1989).
[57] R. C. Newman, *Infrared Studies of Crystal Defects* (Taylor and Francis, London, 1973).
[58] B. Pajot, B. Clerjaud, and Z.J. Xu, Phys. Rev. B **59**, 7500 (1999).
[59] V.P. Markevich, L.I. Murin, J. Hermansson, M. Kleverman, J.L. Lindström, N. Fukata, and M. Suezawa, Physica B **302-303**, 220 (2001).
[60] S.B. Zhang and J.E. Northrup, Phys. Rev. Lett. **67**, 2339 (1991).
[61] S. Pökkö, M.J. Puska, and R.M. Nieminen, Phys. Rev. B **53**, 3813 (1996).
[62] J.E. Northrup, R. Di Felice, and J. Neugebauer, Phys. Rev. B **56**, R4325 (1997).
[63] B. Aradi, A. Gali, P. Deák, J.E. Lowther, N.T. Son, E. Janzén, and W.J. Choyke, Phys. Rev. B **63**, 245202 (2001).
[64] C.G. Van de Walle, Phys. Rev. B **49**, 4579 (1994).
[65] S. D. Smith and W. Taylor, Proc. Phys. Soc. London **79**, 1142 (1962).
[66] H. Sternschulte, K. Thonke, R. Sauer, and S. Koizumi, Phys. Rev. B **59**, 12 924 (1999).
[67] N.M. Johnson, F.A. Ponce, R.A. Street, and R.J. Nemanich, Phys. Rev. B **35**, 4166 (1987).
[68] R. Jones, J. Goss, C. Ewels, and S. Öberg, Phys. Rev. B **50**, 8378 (1994).
[69] G.S. Woods and A.T. Collins, J. Phys. Chem. Solids **44**, 471 (1983).
[70] S. Nakamura, N. Iwasa, M. Senoh, and T. Mukai, Jpn. J. Appl. Phys. **31**, 1258 (1992).
[71] D.M. Kozuch, M. Stavola, S.J. Pearton, C.R. Abernathy, and W.S. Hobson, J. Appl. Phys. **73**, 3716 (1993).
[72] Y. Yamashita, K. Maeda, K. Fujita, N. Usami, K. Suzuki, S. Fukatsu, Y. Mera, and Y. Shiraki, Philos. Mag. Lett. **67**, 165 (1993).
[73] C.P. Ewels, R. Jones, S. Öberg, J. Miro, and P. Deák, Phys. Rev. Lett. **77**, 865 (1996).
[74] P.K. Sitch, R. Jones, S. Öberg, and M.I. Heggie, J. Phys. III **7**, 1381 (1997).
[75] X. Blase, K. Lin, A. Canning, S.G. Louie, and D.C. Chrzan, Chem. Phys. Lett. **84**, 5780 (2000).
[76] M.I. Heggie, S. Jenkins, C.P. Ewels, P. Jemmer, R. Jones, and P.R. Briddon, J. Phys.: Condens. Matter **12**, 10 263 (2000).
[77] J.E. Graebner, M.E. Reiss, L. Seibles, T.M. Hartnett, R.P. Miller, and C.J. Robinson, Phys. Rev. B **50**, 3702 (1994).